

Truncated hierarchical B-splines in isogeometric analysis of thin shell structures

H.R. Atri and S. Shojaee *

Department of Civil Engineering, Shahid Bahonar University of Kerman, Kerman, Iran

(Received May 17, 2017, Revised October 26, 2017, Accepted November 30, 2017)

Abstract. This paper presents an isogeometric discretization of Kirchhoff-Love thin shells using truncated hierarchical B-splines (THB-splines). It is demonstrated that the underlying basis functions are ideally appropriate for adaptive refinement of the so-called thin shell structures in the framework of isogeometric analysis. The proposed approach provides sufficient flexibility for refining basis functions independent of their order. The main advantage of local THB-spline evaluation is that it provides higher degree analysis on tight meshes of arbitrary geometry which makes it well suited for discretizing the Kirchhoff-Love shell formulation. Numerical results show the versatility and high accuracy of the present method. This study is a part of the efforts by the authors to bridge the gap between CAD and CAE.

Keywords: THB-splines; isogeometric analysis; Kirchhoff-Love shell; CAD; CAE

1. Introduction

The isogeometric analysis (IGA) proposed by Hughes *et al.* (2005) is known as one of the most versatile and powerful approaches for solution of complex problems (Seo *et al.* 2010, Shojaee *et al.* 2013, Ivannikov *et al.* 2014, Taheri *et al.* 2014, Kang and Youn 2016, Liu *et al.* 2016, Willberg 2016, Casquero *et al.* 2017). This method offers the possibility of bridging the finite element analysis (FEA) to conventional NURBS-based Computer Aided Design (CAD) tools. In fact, the basic idea behind isogeometric analysis is to utilize the basic functions such as B-splines and NURBS to model exact geometries accurately which invoke the isoparametric concepts to define the unknown field variables for numerical simulations of physical phenomena. NURBS are the most ubiquitous tool in CAD programs and capable of approximating the computational domain, thus they are used as basis functions for analysis. Furthermore, NURBS basis functions possess an intriguing trait; they are typically smooth beyond the classical C^0 -continuity of standard FEM. This advantage makes them more suitable for solving higher order partial differential equations (Tagliabue *et al.* 2014, Dedè and Quarteroni 2015, Bartezzaghi *et al.* 2015) and has been shown to lead in many cases to better accuracy per degree of freedom in contrast to FEM. So far, the finite element method has been increasingly used in many engineering problems, however it has several disadvantages; time consuming procedure for mesh generation and connectivity of elements, low order shape functions which lead to locking phenomena in shell and plate elements; re-meshing in moving boundary

problems and so on. Recently, as an alternative to the FEM, the so-called meshless or meshfree methods have been focused to overcome the drawbacks associated with FEM. However, most of the meshless methods (Liu *et al.* 1995, Liu and Gu 2001, Chen *et al.* 2006, Bui *et al.* 2011, Belytschko *et al.* 1994, Atluri and Zhu 1998) are based on approximation of field variables and do not satisfy Kronecker delta property (Somireddy and Rajagopal 2014). Some researchers have paid great attention to blend advantageous techniques of meshfree approximants and isogeometric analysis, e.g., in Rosolen and Arroyo (2013) local maximum entropy (LME) approximation is coupled with isogeometric analysis. This coupling strategy exploits the best features and overcomes the main drawbacks associated with each of these approximants (Rosolen and Arroyo (2013). In fact, IGA method preserves veracity representation of problem domain boundary and meshfree methods deal with unstructured grids and possibly local refinement. In another research, Valizadeh *et al.* (2015) proposed a methodology based on coupling of isogeometric analysis and Reproducing Kernel Particle Method (RKPM) which is a representative of a class of meshfree methods. The interior domain is discretized by RKPM while IGA provides geometrically exact model discretization. Another meshless method namely Natural Element Method (NEM) developed by Sambridge *et al.* (1995) endows advantageous properties of both meshless and finite element method (Somireddy and Rajagopal 2014). In a research by Gonzalez *et al.* (2008), it is shown that NEM is equivalent to isogeometric analysis. However, this method does not rely on an underlying tensor-product quadrilateral mesh (González *et al.* 2008).

As mentioned above, a considerable attention has been given to circumvent the tensor-product constructions which are expressed in terms of B-spline representation. These

*Corresponding author, Ph.D.,
E-mail: saeed.shojaee@uk.ac.ir

constructions hinder the possibility of accommodating trimmed surfaces, adaptive local refinement, or incongruent surface descriptions at opposing faces. Several different schemes have been developed to provide more flexible solutions that may break the rigidity of classical tensor-product construction imposed by the NURBS framework on the volume meshing. Some of these relevant issues are addressed in T-splines (Sederberg *et al.* 2003, 2004), hierarchical B-splines (Forsey and Bartels 1988), PHT-splines (Li *et al.* 2007), locally refined splines (Dokken *et al.* 2013) and truncated hierarchical B-splines (Giannelli *et al.* 2016).

T-splines are defined by control meshes that allow the introduction of so-called T-junctions. Some researchers have used T-splines in isogeometric analysis (Dörfler *et al.* 2010, Bazilevs *et al.* 2010). Application of T-splines in analysis of thin shells can be found in Uhm and Youn (2009). Since the initial definition of T-splines did not guarantee linear independence (Li *et al.* 2012, Buffa *et al.* 2010), analysis-suitable T-splines (Scott *et al.* 2012) were subsequently introduced to provide this property. However, local refinement in analysis-suitable T-splines may go beyond the domain of interest (Wei *et al.* 2015). In da Veiga *et al.* (2012) and Beirão da Veiga *et al.* (2013), dual-compatible T-splines are proposed and T-splines with linear complexity has been presented in Morgenstern and Peterseim (2015).

Hierarchical B-splines were first introduced by Forsey and Bartels (1988) and had been further elaborated in unther Greiner and Hormann (1996) and Kraft (1997). The classical hierarchical B-splines had suffered from linear independence property which was solved by Kraft (1997). The applications of hierarchical constructions were addressed in Vuong *et al.* (2011), Schillinger *et al.* (2012) and Evans *et al.* (2015). A major drawback of standard hierarchical B-splines is its weakness in providing the partition of unity property. In order to alleviate this disadvantage, a truncated mechanism was developed by Giannelli *et al.* (2012) and in another study by Hughes *et al.* (2015) Truncated Hierarchical Catmull-Clark Subdivision (THCCS) was presented to satisfy partition of unity property.

As reported in Giannelli *et al.* (2012), the truncated basis for hierarchical splines ensures partition of unity, linear independence, and locally refinable. Since THB-splines possess the convex hull property, they are appropriate for geometric modeling and surface reconstructions so they can be used in computer aided design (Kiss *et al.* (2014), additionally, THB-splines are suitable for adaptive numerical solutions, so they can be used as an effective approach in isogeometric analysis. Other applications of THB-splines in modeling of arbitrary topologies and in context of generating systems were reported in Wei *et al.* (2015), Zore and Jüttler (2014).

PHT-splines – a polynomial spline over hierarchical T-meshes, was introduced for stitching several surface patches (Li *et al.* 2007). The basis functions of PHT-splines have the main properties of B-splines, such as non-negativity, local support and partition of unity. They also has the same important property of T-splines like adaptivity (Deng *et al.*

2008). In contrast to T-splines, PHT-splines are polynomial instead of rational and they are only C^1 -continuous which can be mentioned as their main drawback. Compared with hierarchical B-splines, PHT-splines have set of basis functions while hierarchical B-splines have redundant set of basis functions (Deng *et al.* 2008). The applications of PHT-splines in isogeometric analysis can be found in Wang *et al.* (2011) and Nguyen-Thanh *et al.* (2011b). Shell analysis based on PHT-splines was proposed by Nguyen-Thanh *et al.* (2011a).

Locally Refined Splines (LR-splines) are based on splitting the tensor-product of basis functions which lead to challenges with linear independence (Dokken *et al.* 2013) that have been solved in Bressan and Jüttler (2015) and Bressan (2013). Similarities and differences between classical hierarchical, truncated hierarchical and LR B-splines are discussed in Johannessen *et al.* (2015). Local refinement strategies for adaptive isogeometric analysis using LR B-splines are proposed in Johannessen *et al.* (2014). Other geometry representations with application in isogeometric analysis include subdivision surfaces (Cirak *et al.* 2000, 2002) and subdivision solids (Burkhart *et al.* 2010). Subdivision schemes are defined recursively to construct smooth surfaces through the limit of a sequence of refined meshes and they have many practical advantages for shapes of arbitrary topology, e.g., in a study by Cirak *et al.* (2002), subdivision surfaces are proposed as a common foundation for describing the mechanical behavior of thin-shell structures. Wawrzinek *et al.* (2011) employed Catmull-Clark's subdivision (Catmull and Clark 1978) for discretization of Koiter's model of elastic thin shells. A new subdivision algorithm based on IGA that generalizes NURBS to arbitrary topology was presented in Riffnaller-Schiefer *et al.* (2016) for analysis of Kirchhoff-Love thin shells. However, adaptive simulation was not developed for subdivision surfaces in these studies.

The present paper is based on the new concept of THB-splines which was established in Giannelli *et al.* (2012) to investigate the capability of truncated basis functions in analysis of Kirchhoff-Love thin shells by means of showing numerical results on well-known benchmark examples. The main feature of the proposed method is its simplicity and local refinement can be readily accomplished through the refinement of geometric models. The formulation is discretized only by displacement degrees of freedom and there is no need to introduce rotation DOFs due to high continuity of THB-splines.

The structure of this paper is organized as follows:

In Section 2, we state the preliminaries definitions and basic properties of B-splines and review some fundamentals of THB-splines. The isogeometric formulation of thin-shells is briefly derived in Section 3. Numerical examples are presented in Section 4, the goal of this section is to illustrate the performance of the local refinement strategies. In fact, adaptive refinement using truncated hierarchical splines is investigated and compared to the uniform refinement case whether it attains optimal convergence rate due to better accuracy per degrees of freedom. Concluding remarks are drawn in Section 5.

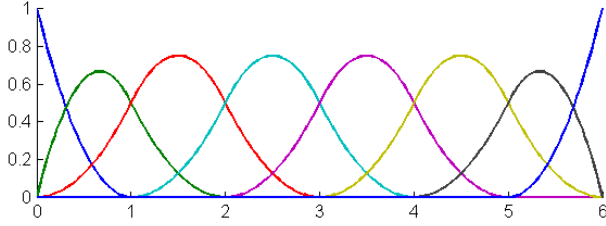


Fig. 1 Quadratic basis functions for open knot vector [0,0,0,1,2,3,4,5,6,6,6]

2. Preliminaries and theory of splines

NURBS are appropriate tools in modeling complex surfaces. In this section, we recall a short description of isogeometric concepts and discuss their implementations.

2.1 B-spline curves and surfaces

A B-spline is a non-interpolating, piecewise polynomial curve. It is defined by a set of control points, \mathbf{P}_i ($i = 1, \dots, n$) and a knot vector $\Xi = \{\xi_1, \xi_2, \dots, \xi_{n+p+1}\}$ where p is the polynomial degree of the curve and n is the number of basis functions corresponding to control points. The knot vector is a non-decreasing sequence of parametric coordinates ξ_i represent points in the parametric space of the curve. Univariate B-spline basis functions are defined recursively using Cox-de Boor formula

$$N_{i,0}(\xi) = \begin{cases} 1 & \text{if } \xi_i \leq \xi \leq \xi_{i+1} \\ 0 & \text{otherwise} \end{cases} \quad (1)$$

and for $p \geq 1$

$$N_{i,p}(\xi) = \frac{\xi - \xi_i}{\xi_{i+p} - \xi_i} N_{i,p-1}(\xi) + \frac{\xi_{i+p+1} - \xi}{\xi_{i+p+1} - \xi_{i+1}} N_{i+1,p-1}(\xi) \quad (2)$$

Fig. 1 shows an example of quadratic basis functions with an open knot vector. B-spline curve of degree p is computed by linear combination of control points and the respective basis functions

$$\mathbf{C}(\xi) = \sum_{i=1}^n N_{i,p}(\xi) \mathbf{P}_i \quad (3)$$

A B-spline surface is computed by the tensor product of B-spline basis functions in two parametric dimensions ξ and η , it is defined by a net of $n \times m$ control points, two knot vectors Ξ and \mathbf{H} , two polynomial degrees p and q (not necessary to be equal), and correspondingly basis functions $N_{i,p}(\xi)$ and $M_{j,q}(\eta)$ described as

$$\mathbf{S}(\xi, \eta) = \sum_{i=1}^n \sum_{j=1}^m N_{i,p}(\xi) M_{j,q}(\eta) \mathbf{P}_{i,j} \quad (4)$$

2.2 NURBS

For a NURBS curve, each control point has an individual weight w_i , such a point \mathbf{P}_i (x_i, y_i, z_i, w_i) can be represented with homogeneous coordinates \mathbf{P}_i ($w_i x_i, w_i y_i,$

$w_i z_i, w_i$) in a projective R^4 space. Similarly to B-spline curves and surfaces, NURBS-based ones are defined as

$$\mathbf{C}(\xi) = \frac{\sum_{i=1}^n N_{i,p}(\xi) w_i \mathbf{P}_i}{\sum_{j=1}^n N_{j,p}(\xi) w_j} \quad (5)$$

$$\mathbf{S}(\xi, \eta) = \frac{\sum_{i=1}^n \sum_{j=1}^m N_{i,p}(\xi) M_{j,q}(\eta) w_{i,j} \mathbf{P}_{i,j}}{\sum_{k=1}^n \sum_{l=1}^m N_{k,p}(\xi) M_{l,q}(\eta) w_{k,l}} \quad (6)$$

2.3 Hierarchical B-splines

According to Eq. (2), univariate B-spline basis functions $N_{i,p}(\xi)$ defined on a knot vector $\Xi = \{\xi_1, \xi_2, \dots, \xi_{n+p+1}\}$ with a local support on $[\xi_i, \xi_{i+p+1}]$ are refinable which allows local refinement and construction of hierarchical B-splines. Let Ω^0 is the parametric domain of all basis functions $N_{i,p}^0$ defined on initial knot vector Ξ^0 at level 0. B-spline basis functions $N_{i,p}^l$ associated with level l is obtained by subdividing the knot vector of previous level. Therefore, the basis functions $N_{i,p}^l$ on level l can be written as a linear combination of $p+2$ basis functions $N_{i,p}^{l+1}$ defined on Ξ^{l+1} Bornemann and Cirak (2013)

$$N_{i,p}^l(\xi) = \sum_{r=0}^{p+1} \alpha_r^p N_{2i+r,p}^{l+1}(\xi) \quad \text{with } \alpha_r^p = \frac{1}{2^p} \binom{p+1}{r} \quad (7)$$

where α_r^p are binomial coefficients. The B-splines $N_{2i+r,p}^{l+1}(\xi)$ defined on the refined knot sequence are called the children of $N_{i,p}^l$. Similar to univariate basis functions, a bivariate B-spline basis $N_{i,p}(\xi, \eta)$ defined by a tensor product of two univariate basis functions with polynomial degrees p and q has local support $[\xi_i, \xi_{i+p+1}] \times [\eta_j, \eta_{j+q+1}]$ with $(p+2) \times (q+2)$ children. The hierarchical B-spline refinement can be achieved by replacing coarse grid B-spline basis with fine ones. The process is briefly illustrated as follows: Let N^l be the tensor product of B-spline basis at level l defined on parametric domain Ω^l in which the union of $\text{supp} N_{i,p}^l(\xi, \eta)$ equals Ω^l . Suppose $\mathcal{N} \in N^0$ and $\text{supp } \mathcal{N} \neq \emptyset$. Then find a set of basis functions $\mathcal{N} \in N^l$ in such way that $\text{supp } \mathcal{N} \subset \Omega^{l+1}$. Next, identify the children of \mathcal{N} at level $l+1$, so that $\mathcal{N} \in N^{l+1}$ and $\text{supp } \mathcal{N} \subseteq \Omega^{l+1}$. Finally gather all the active basis functions at levels l and $l+1$ as follows

$$\begin{aligned} \mathfrak{H} &= \left\{ \mathcal{N} \in N^l : \text{supp } \mathcal{N} \subset \Omega^{l+1} \right\} \\ &\cup \left\{ \mathcal{N} \in N^{l+1} : \text{supp } \mathcal{N} \subseteq \Omega^{l+1} \right\} \quad (8) \\ &\text{for } \ell = 0, \dots, \ell_{\max} - 1 \end{aligned}$$

Eq. (8) is the recursive construction of hierarchical B-splines which are globally linearly independent (Kraft 1997). Hierarchical B-splines do not ensure partition of unity. Moreover, different hierarchical levels cause increasing the number of overlapping basis functions during the local refinement which leads bad numerical conditioning and may produce ill-shaped control meshes at the refined

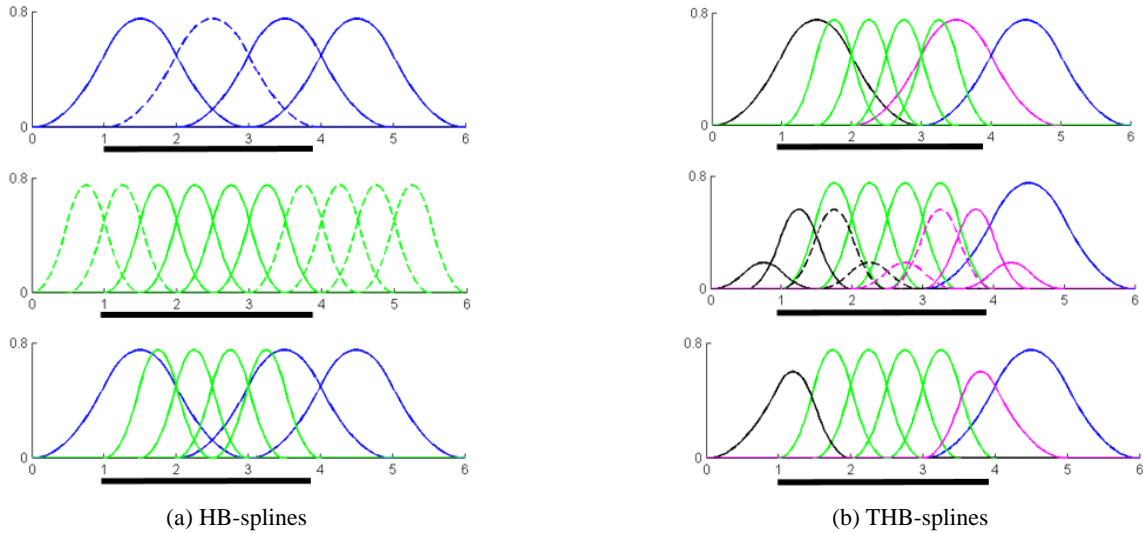


Fig. 2 The procedure to form univariate quadratic HB- and THB-splines (a)-(b). For case (a), top: the blue dashed curve is designated as passive basis function; middle: the green solid curves are designated as active; bottom: the combination of active basis functions from two previous levels to construct the hierarchical B-splines. For case (b), top: the hierarchical B-splines of level 0 that need to be truncated or modified are depicted in black and magenta curves; middle: the four children of each mentioned curves are shown and the children with supports fully contained in black area are discarded; bottom: the remaining active basis functions are collected to construct THB-splines

level (Wei *et al.* 2015). To overcome the drawbacks of hierarchical B-splines, another basis termed truncated hierarchical B-splines was presented (Giannelli *et al.* 2012).

2.4 Truncated hierarchical B-splines

Truncated hierarchical B-splines (THB-splines) based on the truncation operation of hierarchical splines was first introduced by Giannelli *et al.* 2012. THB-splines have a bifold motivation. On the one hand, they are natural extension of classical B-splines with similar properties such as partition of unity, non-negativity, convex hull and compact support, on the other hand, the locality of the refinement they provide has smaller support than hierarchical B-splines. The construction process of THB-splines is analogous to hierarchical B-splines with just one difference; the basis functions $\mathcal{N} \in N^l$ with $\text{supp } \mathcal{N} \not\subset \Omega^{l+1}$ should be truncated. The truncated mechanism can be expressed as follows.

Definition. According to Eq. (7), a set of basis functions $\mathbf{t} \subseteq \Omega^l$ can be represented with respect to the finer basis of $\mathcal{N} \in N^{l+1}$

$$\mathbf{t} = \sum_{\mathcal{N} \in N^{l+1}} \alpha_{\mathcal{N}}^{\ell+1} \mathcal{N}, \quad \alpha_{\mathcal{N}}^{\ell+1} \in \mathbb{R} \quad (9)$$

The truncated basis functions of \mathbf{t} with respect to N^{l+1} is expressed as

$$\text{trunc}^{\ell+1} \mathbf{t} = \sum_{\mathcal{N} \in N^{l+1}, \text{supp } \mathcal{N} \not\subset \Omega^{l+1}} \alpha_{\mathcal{N}}^{\ell+1} \mathcal{N}, \quad \alpha_{\mathcal{N}}^{\ell+1} \in \mathbb{R} \quad (10)$$

In fact for THB-splines, the children of coarse basis functions whose support have a non-empty overlap with

Ω^{l+1} are discarded. Iterative construction process of univariate hierarchical and truncated hierarchical B-splines for two levels is shown in Fig. 2. First, consider the univariate B-spline basis functions at level 0 as coarse basis (Fig. 1) and fine ones at level 1 with knot vector $\left[0, 0, 0, \frac{1}{12}, \frac{2}{12}, \dots, \frac{10}{12}, \frac{11}{12}, 1, 1, 1\right]$. The parameter domain for level 0 is referred to as Ω^0 and the black area in the picture indicating $\Omega^1 \subset \Omega^0$ is the area needs to be refined. The coarse basis function with support fully contained in the black area and all fine basis functions whose support are not in Ω^1 are depicted as dashed curves and known as passive basis (Fig. 2. (a)-top and middle). By taking the union of all the active basis functions (solid curves) from levels 0 and 1, the hierarchical B-spline basis of level 1 can be obtained. (Fig. 2. (a)-bottom). For THB-splines, the remaining active coarse basis functions surrounding the passive ones should be truncated. For this purpose, two basis functions adjacent to the blue dashed curve (magenta and black curves) can be represented by their children. Among the children, those with supports fully contained in Ω^1 should be discarded (the black and magenta dashed curves) and the remaining children are designated as active (Fig. 2. (b)-middle), by collecting all the active basis functions from levels 0 and 1, the truncated hierarchical B-splines can be constructed (Fig. 2. (b)-bottom).

In contrast to hierarchical splines, THB-splines are strongly stable which is implied by partition of unity and sparser connectivity. In addition, the geometry is preserved during the local refinement. Assume $S(\xi)$ is a certain spline geometry (curve, surface, and volume) represented by tensor product splines of level l with control points P_i^l according to Eq. (3), (4) or (5)

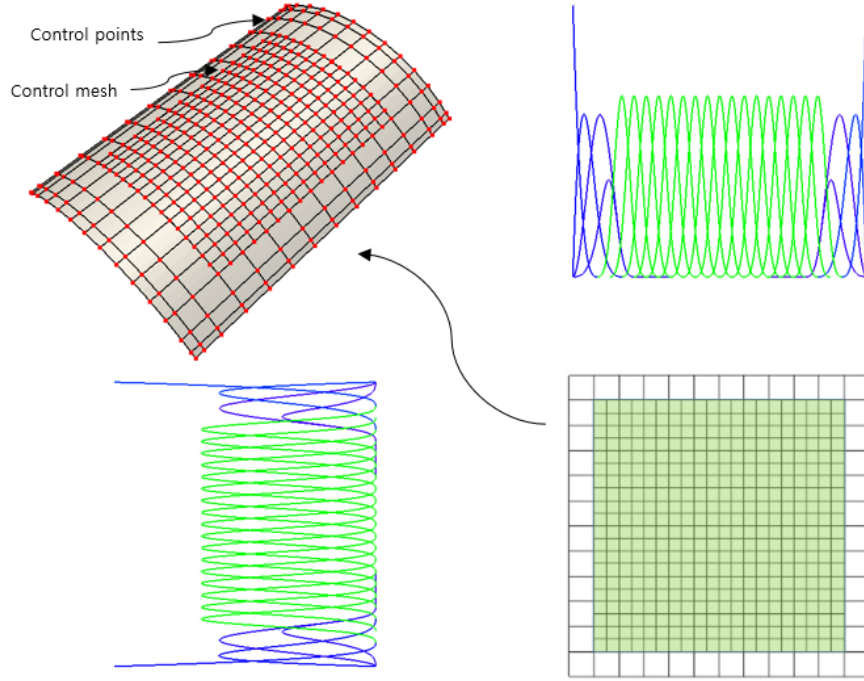


Fig. 3 THB-spline representation of a roof using hierarchical meshes in the parameter domain: (top-left) the geometry with refined control points; (bottom-right) the corresponding hierarchical mesh in the parameter domain, the shaded box (green) is the refined area with its corresponding basis functions in two directions

$$S(\xi) = \sum_{\mathcal{N}_i^\ell \in \mathcal{N}^\ell} P_i^\ell \mathcal{N}_i^\ell(\xi) \quad (11)$$

The same geometry can be represented on level $l+1$ with different control points P_j^{l+1}

$$S(\xi) = \sum_{\mathcal{N}_j^{l+1} \in \mathcal{N}^{l+1}} P_j^{l+1} \mathcal{N}_j^{l+1}(\xi) \quad (12)$$

The hierarchical B-spline basis with truncation can be obtained consisting of only those coarse function \mathcal{N}_i^ℓ where $\text{supp } \mathcal{N}_i^\ell \subset \Omega^\ell \wedge \text{supp } \mathcal{N}_i^\ell \not\subset \Omega^{\ell+1}$ and fine functions \mathcal{N}_j^{l+1} where $\text{supp } \mathcal{N}_j^{l+1} \subset \Omega^{\ell+1}$. The spline geometry can be represented exactly by taking the same control points P_i^ℓ and P_j^{l+1} that are used on the respective level.

$$S(\xi) = \sum_{\substack{\mathcal{N}_i^\ell \in \mathcal{N}^\ell \\ \text{supp } \mathcal{N}_i^\ell \not\subset \Omega^{\ell+1}}} P_i^\ell \mathcal{N}_i^\ell(\xi) + \sum_{\substack{\mathcal{N}_j^{l+1} \in \mathcal{N}^{l+1} \\ \text{supp } \mathcal{N}_j^{l+1} \subset \Omega^{\ell+1}}} P_j^{l+1} \mathcal{N}_j^{l+1}(\xi) \quad (13)$$

An example of a cubic B-spline surface with truncation is represented in Fig. 3. The control points are shown in red and the control mesh exhibits T-joints on the surface.

3. Review of thin shell equations

Thin shell structures appear ubiquitously in nature and technology and they have great applications in many areas of applied engineering design. Since one dimension of a thin shell is small with respect to the two others, its geometry can be described in terms of the middle surface of a shell. Thus, two manifold meshes are required to simulate

thin shell structures. The mechanical behavior of a thin shell can be described by Kirchhoff-Love theory in terms of the first and second fundamental forms of surfaces. In the Kirchhoff-Love shell theory, shell cross sections are assumed to remain normal to its mid-surface during deformation which implies linear strain distribution through the thickness and neglects transverse shear strains. In the following, the fundamental concepts of shells are considered. A detailed description of classical shell theories can be found in Flügge and Truesdell (1972). Our discretized thin shell formulation closely follows Naghdi's approach, but it is extended to truncated hierarchical B-splines.

3.1 Kirchhoff-Love thin shell formulation

The geometry of a shell can be characterized by its undeformed middle surface Ω and boundary $\Gamma = \partial\Omega$. The deformed configuration of the shell under the action of applied loads is defined by a surface of a domain $\bar{\Omega}$ and boundary $\bar{\Gamma} = \partial\bar{\Omega}$. The shell geometry with thickness h in the reference configuration in terms of curvilinear coordinates $(\theta_1, \theta_2, \theta_3)$ is given by

$$P(\theta_1, \theta_2, \theta_3) = X(\theta_1, \theta_2) + \theta_3 \mathbf{a}_3, \quad -\frac{h}{2} \leq \theta_3 \leq \frac{h}{2} \quad (14)$$

where P is the position vector of a material point and $X(\theta_1, \theta_2)$ specifies position vector to each point on the middle surface of the shell. The shell director \mathbf{a}_3 is the unit normal vector to the midsurface. The corresponding basis vectors in the reference configuration are expressed as

$$\mathbf{a}_\alpha = \mathbf{X}_{,\alpha}, \quad \alpha \in \{1, 2\} \quad (15)$$

where the comma indicates the partial derivative with respect to θ_α . The covariant basis vectors of the tangent plane are as follows

$$\mathbf{g}_\alpha = \frac{\partial \mathbf{P}}{\partial \theta_\alpha} = \mathbf{a}_\alpha + \theta_3 \mathbf{a}_{3,\alpha} \quad (16)$$

$$\text{with } \mathbf{g}_3 = \mathbf{a}_3 \text{ and } \alpha \in \{1, 2\}$$

According to the first fundamental form of the surface, the covariant components of the surface metric tensor in the reference configuration are defined as

$$a_{\alpha\beta} = \mathbf{a}_\alpha \cdot \mathbf{a}_\beta \quad \alpha, \beta \in \{1, 2\} \quad (17)$$

whereas the covariant components of the curvature tensors based on the second fundamental form are given as

$$b_{\alpha\beta} = \mathbf{a}_{\alpha,\beta} \cdot \mathbf{a}_3 \quad \alpha, \beta \in \{1, 2\} \quad (18)$$

We define the following strain tensor by means of the well-known formula

$$\mathbf{E} = E_{\alpha\beta} \cdot \mathbf{g}^\alpha \times \mathbf{g}^\beta \quad \text{with } E_{\alpha\beta} = \varepsilon_{\alpha\beta} + \xi_3 \varphi_{\alpha\beta} \quad (19)$$

where \mathbf{g}^α and \mathbf{g}^β are contravariant basis vectors. Two strains; ε or membrane strains for describing the straining of the surface and φ or bending strains for measuring the change in curvature of the shell are expressed as

$$\varepsilon_{\alpha\beta} = \frac{1}{2} (\bar{a}_{\alpha\beta} - a_{\alpha\beta}) \quad (20)$$

$$\varphi_{\alpha\beta} = \bar{b}_{\alpha\beta} - b_{\alpha\beta} \quad (21)$$

The deformed geometry of the shell can be described by

$$\bar{\mathbf{X}}(\theta_1, \theta_2) = \mathbf{X}(\theta_1, \theta_2) + \mathbf{u}(\theta_1, \theta_2) \quad (22)$$

The linearized membrane and bending strains with the aid of Eq. (22) can be rewritten as

$$\varepsilon_{\alpha\beta} = \frac{1}{2} (\mathbf{a}_{\alpha,\beta} \cdot \mathbf{u}_\beta - \mathbf{u}_\alpha \cdot \mathbf{a}_{\beta,\alpha}) \quad (23)$$

$$\begin{aligned} \varphi_{\alpha\beta} = & -\mathbf{u}_{,\alpha\beta} \cdot \mathbf{a}_3 + \frac{1}{\sqrt{a}} [\mathbf{u}_{,1} \cdot (\mathbf{a}_{\alpha,\beta} \times \mathbf{a}_2) + \mathbf{u}_{,2} \cdot (\mathbf{a}_1 \times \mathbf{a}_{\alpha,\beta})] \\ & + \frac{\mathbf{a}_3 \cdot \mathbf{a}_{\alpha,\beta}}{\sqrt{a}} [\mathbf{u}_{,1} \cdot (\mathbf{a}_2 \times \mathbf{a}_3) + \mathbf{u}_{,2} \cdot (\mathbf{a}_3 \times \mathbf{a}_1)] \end{aligned} \quad (24)$$

For simplicity, it is assumed that the shell is linearly elastic and its strain energy density per unit area is expressed as

$$\begin{aligned} W(\mathbf{u}) = & \frac{1}{2} \frac{Et}{1-\nu^2} C^{\alpha\beta\gamma\delta} \varepsilon_{\alpha\beta} \varepsilon_{\gamma\delta} \\ & + \frac{1}{2} \frac{Et^3}{12(1-\nu^2)} C^{\alpha\beta\gamma\delta} \varphi_{\alpha\beta} \varphi_{\gamma\delta} \\ = & \frac{1}{2} \mathbf{D}_m \varepsilon_{\alpha\beta} \varepsilon_{\gamma\delta} + \frac{1}{2} \mathbf{D}_b \varphi_{\alpha\beta} \varphi_{\gamma\delta} \end{aligned} \quad (25)$$

where ν and E denote Poisson's ratio and modulus of elasticity, respectively. The fourth order constitutive tensor $C^{\alpha\beta\gamma\delta}$ is defined by

$$C^{\alpha\beta\gamma\delta} = \nu a^{\alpha\beta} a^{\gamma\delta} + \frac{1}{2} (1-\nu) (a^{\alpha\gamma} a^{\beta\delta} + a^{\alpha\delta} a^{\beta\gamma}) \quad (26)$$

with $\alpha^{\alpha\beta}$ as the contravariant components of the surface metric tensor. Membrane strains in the framework of finite element approximation of the displacement field can be rewritten as follows

$$\begin{bmatrix} \varepsilon_{11} \\ \varepsilon_{22} \\ 2\varepsilon_{12} \end{bmatrix} = \begin{bmatrix} \mathbf{a}_1 \cdot \mathbf{R}_{l,1} \\ \mathbf{a}_2 \cdot \mathbf{R}_{l,2} \\ \mathbf{a}_1 \cdot \mathbf{R}_{l,2} + \mathbf{a}_2 \cdot \mathbf{R}_{l,1} \end{bmatrix} \mathbf{u}_l \quad (27)$$

In compact form

$$\varepsilon = \mathbf{B}_l^m \mathbf{u}_l \quad (28)$$

where \mathbf{B}_l^m is the membrane strain-displacement matrix. In the same manner, bending strain-displacement can be derived as

$$\begin{bmatrix} \varphi_{11} \\ \varphi_{22} \\ 2\varphi_{12} \end{bmatrix} = \begin{bmatrix} \mathbf{B}_{1l} \\ \mathbf{B}_{2l} \\ \mathbf{B}_{3l} \end{bmatrix} \mathbf{u}_l = \mathbf{B}_l^b \mathbf{u}_l \quad (29)$$

in which

$$\begin{aligned} \mathbf{B}_{1l} = & -R_{l,11} \mathbf{a}_3 + \frac{1}{\|\mathbf{a}_1 \times \mathbf{a}_2\|} [R_{l,1} \cdot (\mathbf{a}_{1,1} \times \mathbf{a}_2) + R_{l,2} \cdot (\mathbf{a}_{1,1} \times \mathbf{a}_1)] \\ & + \frac{\mathbf{a}_3 \cdot \mathbf{a}_{1,1}}{\|\mathbf{a}_1 \times \mathbf{a}_2\|} [R_{l,1} \cdot (\mathbf{a}_2 \times \mathbf{a}_3) + R_{l,2} \cdot (\mathbf{a}_3 \times \mathbf{a}_1)] \end{aligned} \quad (30a)$$

$$\begin{aligned} \mathbf{B}_{2l} = & -R_{l,22} \mathbf{a}_3 + \frac{1}{\|\mathbf{a}_1 \times \mathbf{a}_2\|} [R_{l,1} \cdot (\mathbf{a}_{2,2} \times \mathbf{a}_2) + R_{l,2} \cdot (\mathbf{a}_{2,2} \times \mathbf{a}_1)] \\ & + \frac{\mathbf{a}_3 \cdot \mathbf{a}_{2,2}}{\|\mathbf{a}_1 \times \mathbf{a}_2\|} [R_{l,1} \cdot (\mathbf{a}_2 \times \mathbf{a}_3) + R_{l,2} \cdot (\mathbf{a}_3 \times \mathbf{a}_1)] \end{aligned} \quad (30b)$$

$$\begin{aligned} \mathbf{B}_{3l} = & -2R_{l,12} \mathbf{a}_3 + \frac{2}{\|\mathbf{a}_1 \times \mathbf{a}_2\|} [R_{l,1} \cdot (\mathbf{a}_{1,2} \times \mathbf{a}_2) + R_{l,2} \cdot (\mathbf{a}_{1,2} \times \mathbf{a}_1)] \\ & + 2 \frac{\mathbf{a}_3 \cdot \mathbf{a}_{1,2}}{\|\mathbf{a}_1 \times \mathbf{a}_2\|} [R_{l,1} \cdot (\mathbf{a}_2 \times \mathbf{a}_3) + R_{l,2} \cdot (\mathbf{a}_3 \times \mathbf{a}_1)] \end{aligned} \quad (30c)$$

where subscript l indicates number of control points and R is truncated hierarchical B-splines and its derivatives.

By applying the internal virtual work we have

$$\begin{aligned} \delta W_{\varepsilon_m} = & \int_{\Omega} \delta \boldsymbol{\varphi}^T \mathbf{D}_m + \delta \boldsymbol{\varphi}^T \mathbf{D}_b \boldsymbol{\varphi} d\Omega \\ = & \delta \mathbf{u}_l^T \int_{\Omega} [(\mathbf{B}_l^m)^T \mathbf{D}_m \mathbf{B}_l^m + (\mathbf{B}_l^b)^T \mathbf{D}_b \mathbf{B}_l^b] d\Omega \mathbf{u}_l \end{aligned} \quad (31)$$

For convenience of computer programming, the element stiffness matrix is given as follows

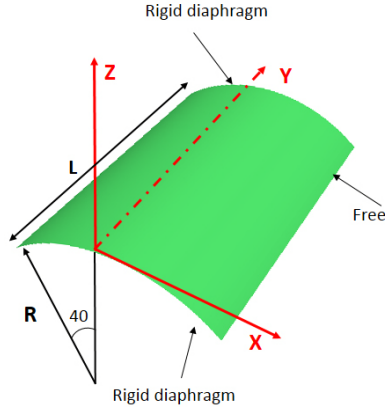


Fig. 4 Scordelis-Lo roof

$$\mathbf{K}_e = \int_{\Omega} [(\mathbf{B}_e^m)^T \mathbf{D}_m \mathbf{B}_e^m + (\mathbf{B}_e^b)^T \mathbf{D}_b \mathbf{B}_e^b] d\Omega \quad (32)$$

In the present study, the standard Gauss quadrature is carried out on knot spans and the numerical results are obtained using $(p+1)(q+1)$ Gauss points in shell elements, where p and q are the orders of truncated basis functions. As the basis functions are rational polynomials, Gaussian quadrature seems to be credible for integrating them.

4. Numerical results

In this section, the performance and the accuracy of our implementation of an isogeometric thin shell element based on truncated hierarchical basis are investigated. We show the efficiency and versatility of the proposed method through three benchmark problems taken from the well-known shell obstacle course (Belytschko 1985): the Scordelis-Lo roof, the pinched cylinder and the hemispherical shell. The present results are compared with analytical solutions and those of the original NURBS approach. At level 0, our results are equivalent to those derived with cubic NURBS.

4.1 Scordelis-Lo roof

Consider the Scordelis-Lo roof shown in Fig. 4 as a panel of cylindrical shell with self-weight ($q = 90/area$) that is supported at its ends by rigid diaphragms and the other two edges are free. The vertical displacement at the midpoint of the side edge is given as the reference solution (Belytschko 1985). Geometric and material data are assumed as follows: the radius of roof $R = 25$; its length $L = 50$; the thickness $t = 0.25$; the modulus of elasticity $E = 4.32 \times 10^8$; and the Poisson's ratio $\nu = 0.0$. Taking advantage of symmetry enables us to model and analyze only one quadrant of the roof. Hierarchical meshes are constructed

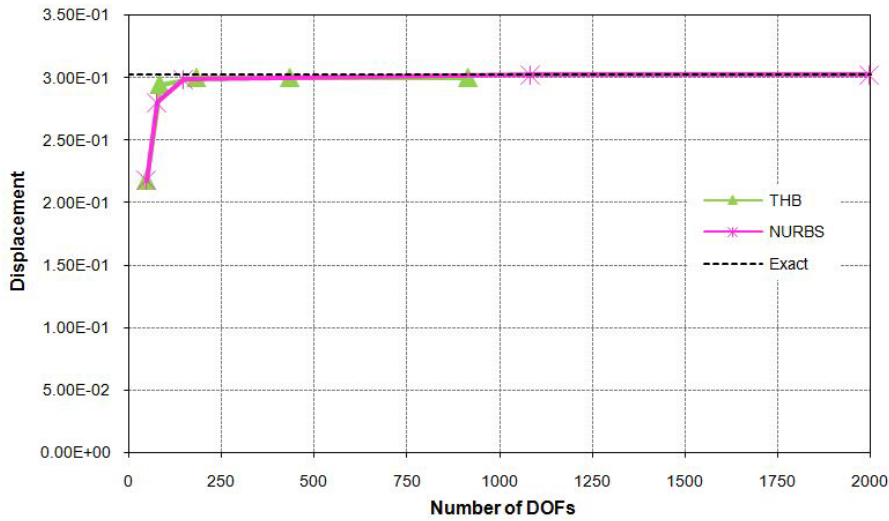


Fig. 5 Scordelis-Lo roof, vertical displacement at the midpoint of free edge

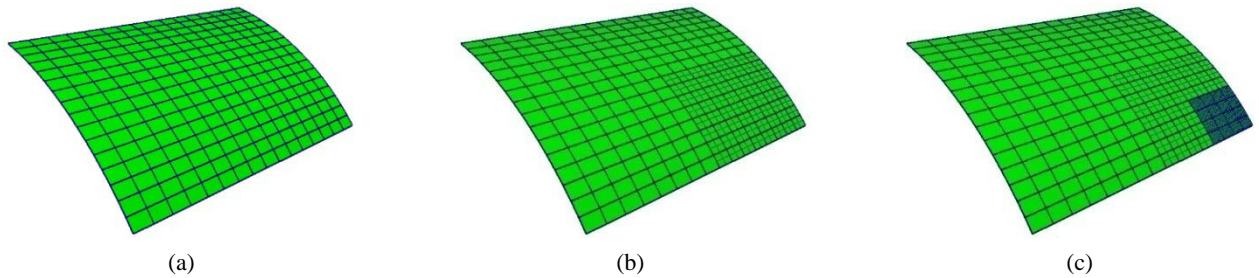


Fig. 6 Physical mesh of Scordelis-Lo roof: (a) a uniformly coarse mesh for both NURBS and THB-splines at level 0; (b) slightly finer meshes for THB-splines at level 1; (c) fine meshes for THB-splines at level 2



Fig. 7 Scordelis-Lo roof, vertical displacement at the midpoint of free edge

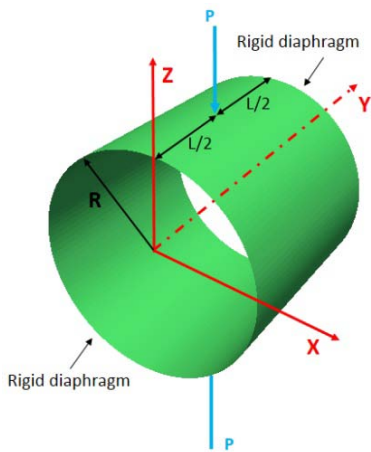


Fig. 8 Pinched cylinder with end diaphragms

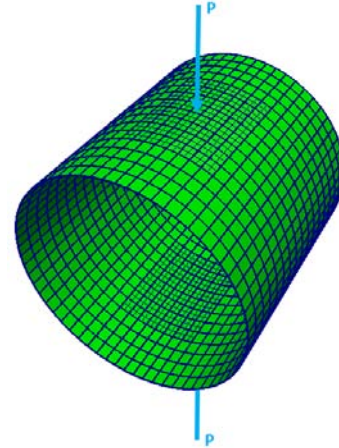


Fig. 10 Local refinement representation of pinched cylinder at loading points

for three different levels (see Fig. 6).

The numerical convergence of methods are also plotted in Fig. 5. The maximum value of the vertical displacement calculated at the midpoint of free edge using THB-splines is a little lower than the exact value. This slight difference is due to neglecting transverse shear deformation, because the present formulation is based on Kirchhoff-Love theory while in the reference solution, shear deformations are included. As can be seen in Fig. 5, the convergence rate of truncated hierarchical B-splines appear satisfactory. Moreover, THB-splines exhibit more accurate solution with

respect to lower degrees of freedoms than NURBS model when the same order approximation is used. Contour plot of vertical deflection at the center of the free edge and the deformed configuration are shown in Fig. 7.

4.2 Pinched cylinder with end diaphragms

In this section, a pinched cylinder with rigid end diaphragms and two opposite concentrated point loads ($P = 1.0$) is considered. The simulated material has a uniform thickness of $t = 3$, Young's modulus is $E = 3.0 \times 10^6$ and

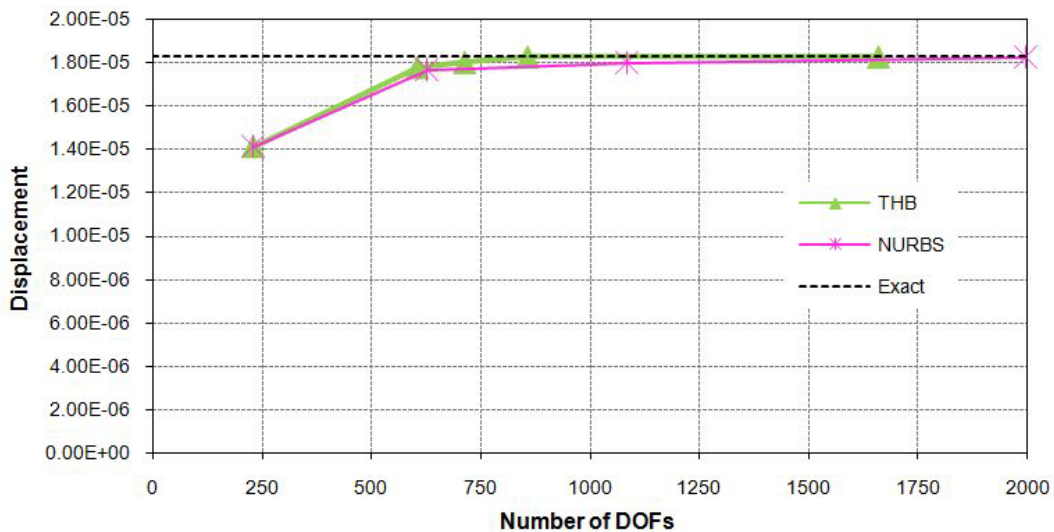


Fig. 9 Displacement convergence plot of pinched cylinder

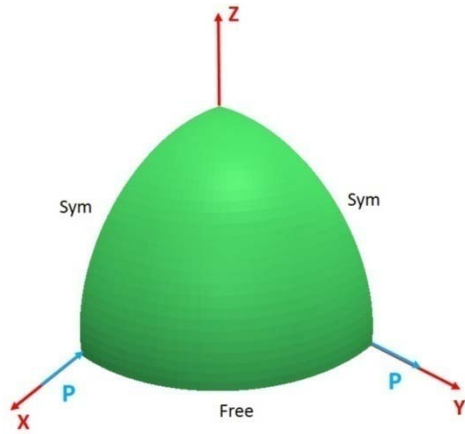


Fig. 11 Quadrant of a pinched hemispherical shell

Poisson's ratio is $\nu = 0.3$. Geometrical parameters are as follows: the radius of cylinder $R = 25$ and its length $L = 50$. The theoretical solution of the expected deflection under the loading point is 1.8248×10^{-5} (Belytschko *et al.* 1985). Fig. 8 describes the geometry of the problem. The full model of pinched cylinder with local refinement under the point loads is depicted in Fig. 10.

Owing to symmetry, one octant of the pinched cylinder is modeled by cubic NURBS basis functions. Fig. 9 depicts the convergence of the radial displacement at the loading point.

It is observed that THB-splines yield more rapidly converging solution to theoretical value. The plot also shows that NURBS basis functions have monotonic convergence towards the reference solution but it is particularly interesting to point out that THB-splines have lower degrees of freedom in contrast to NURBS.

4.3 Hemispherical shell

Fig. 11 shows a quadrant of a pinched hemispherical shell subjected to two opposite diametrical loads $P = 1.0$ in the equatorial plane. The bottom circumferential edge of hemisphere is free. This problem is known as a test for the

performance of the element to handle rigid body rotation about the normal to the shell surface. The parameters are given as follows: the radius of shell $R = 10$; the thickness $t = 0.04$; the modulus of elasticity $E = 6.825 \times 10^7$; and the Poisson's ratio $\nu = 0.3$. The theoretical value for the radial displacement at loading points is 0.0924. Fig. 12 depicts convergence of radial displacement for both NURBS with uniform refinement and THB-splines with local refinement at loading points. It is observed that, the performance of truncated hierarchical constructions is in excellent agreement with the analytical solution. Control mesh of hemispherical shell with its corresponding parameter domain with respect to different degrees of freedom are illustrated in Fig. 13. Contour plot of displacement at loading points is depicted in Fig. 14.

5. Conclusions

In this paper, the hierarchical B-splines with truncation was applied for analysis of thin shell structures in the framework of isogeometric approach. The analysis has been carried out using different levels of hierarchical meshes. Due to high continuity of THB-splines, only displacement degrees of freedom were discretized. Therefore, the number of DOFs are lower because not only the local refinement is implemented but also the middle surface of a rotation-free thin shell is modelled. The proposed approach provides sufficient flexibility for preserving the exact geometry representation throughout the refinement process. Hence, it should be mentioned that, the isogeometric analysis using THB-splines exploits refinability of basis functions and can be suggested as a promising alternative to the current geometric modeling and isogeometric analysis.

References

- Atluri, S.N. and Zhu, T. (1998), "A new meshless local Petrov-Galerkin (MLPG) approach in computational mechanics", *Computat. Mech.*, **22**(2), 117-127.

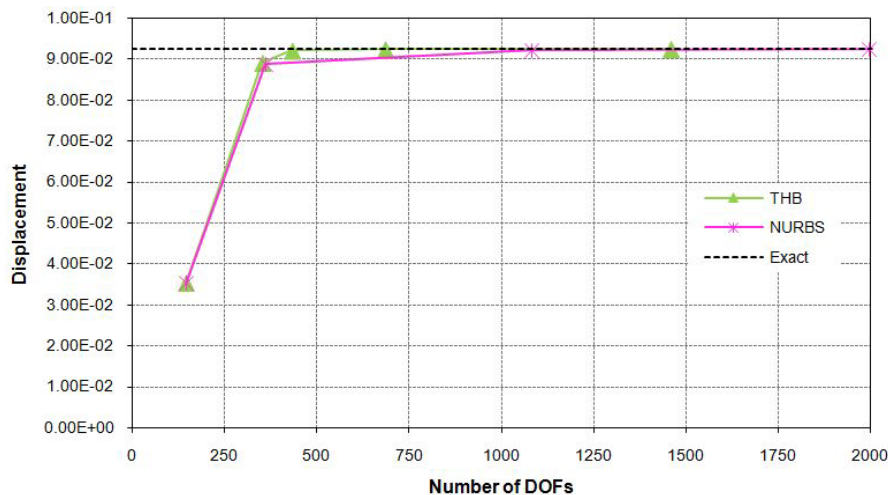


Fig. 12 Displacement convergence of pinched hemispherical shell at loading points

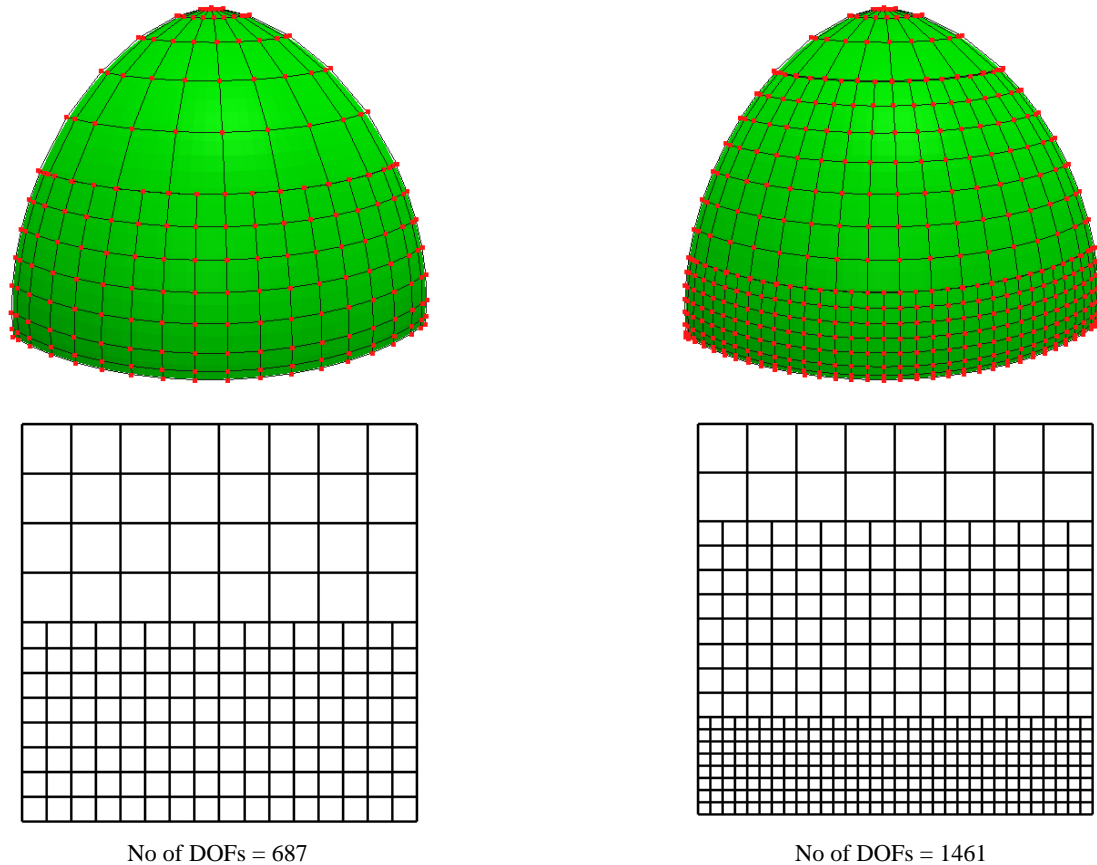


Fig. 13 THB-spline representation of hemispherical shell. Control meshes (top row) and corresponding hierarchical meshes in the parameter domain (bottom row) for two different levels

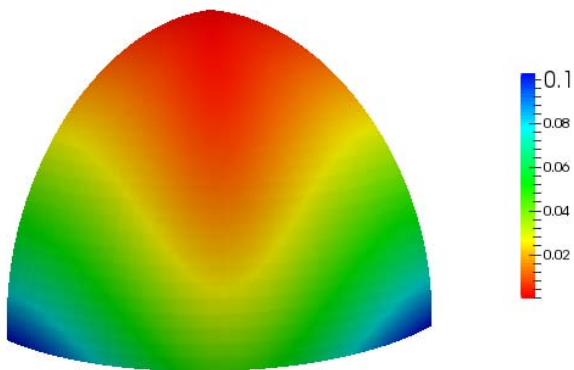


Fig. 14 Contour plot of displacement at loading points of a hemispherical shell

- Bartezzaghi, A., Dedè, L. and Quarteroni, A. (2015), "Isogeometric analysis of high order partial differential equations on surfaces", *Comput. Methods Appl. Mech. Eng.*, **295**, 446-469.
- Bazilevs, Y., Calo, V.M., Cottrell, J.A., Evans, J.A., Hughes, T., Lipton, S., Scott, M.A. and Sederberg, T.W. (2010), "Isogeometric analysis using T-splines", *Comput. Methods Appl. Mech. Eng.*, **199**(5), 229-263.
- Beirão da Veiga, L., Buffa, A., Sangalli, G. and Vázquez, R. (2013), "Analysis-suitable T-splines of arbitrary degree: definition, linear independence and approximation properties", *Math. Models Methods Appl. Sci.*, **23**(11), 1979-2003.
- Belytschko, T., Stolarski, H., Liu, W.K., Carpenter, N. and Ong,

- J.S. (1985), "Stress projection for membrane and shear locking in shell finite elements", *Comput. Methods Appl. Mech. Eng.*, **51**, 221-258.
- Belytschko, T., Lu, Y.Y. and Gu, L. (1994), "Element-free Galerkin methods", *Int. J. Numer. Methods Eng.*, **37**(2), 229-256.
- Bornemann, P. and Cirak, F. (2013), "A subdivision-based implementation of the hierarchical b-spline finite element method", *Comput. Methods Appl. Mech. Eng.*, **253**, 584-598.
- Bressan, A. (2013), "Some properties of LR-splines", *Comput. Aid. Geomet. Des.*, **30**, 778-794.
- Bressan, A. and Jüttler, B. (2015), "A hierarchical construction of LR meshes in 2D", *Comput. Aid. Geomet. Des.*, **37**, 9-24.
- Buffa, A., Cho, D. and Sangalli, G. (2010), "Linear independence of the T-spline blending functions associated with some particular T-meshes", *Comput. Methods Appl. Mech. Eng.*, **199**(23), 1437-1445.
- Bui, T.Q., Nguyen, M.N. and Zhang, C. (2011), "An efficient meshfree method for vibration analysis of laminated composite plates", *Computat. Mech.*, **48**(2), 175-193.
- Burkhart, D., Hamann, B. and Umlauf, G. (2010), "Iso-geometric Finite Element Analysis Based on Catmull-Clark: subdivision Solids", In: *Computer Graphics Forum*, Wiley Online Library, pp. 1575-1584.
- Casquero, H., Liu, L., Zhang, Y., Reali, A., Kiendl, J. and Gomez, H. (2017), "Arbitrary-degree T-splines for isogeometric analysis of fully nonlinear Kirchhoff-Love shells", *Comput.-Aid. Des.*, **82**, 140-153.
- Catmull, E. and Clark, J. (1978), "Recursively generated B-spline surfaces on arbitrary topological meshes", *Comput.-Aid. Des.*, **10**, 350-355.

- Chen, Y., Lee, J. and Eskandarian, A. (2006), *Meshless Methods in Solid Mechanics*, Springer Science & Business Media.
- Cirak, F., Ortiz, M. and Schroder, P. (2000), "Subdivision surfaces: a new paradigm for thin-shell finite-element analysis", *Int. J. Numer. Methods Eng.*, **47**, 2039-2072.
- Cirak, F., Scott, M.J., Antonsson, E.K., Ortiz, M. and Schröder, P. (2002), "Integrated modeling, finite-element analysis, and engineering design for thin-shell structures using subdivision", *Comput.-Aid. Des.*, **34**, 137-148.
- da Veiga, L.B., Buffa, A., Cho, D. and Sangalli, G. (2012), "Analysis-suitable T-splines are dual-compatible", *Comput. Methods Appl. Mech. Eng.*, **249**, 42-51.
- Dedè, L. and Quarteroni, A. (2015), "Isogeometric Analysis for second order partial differential equations on surfaces", *Comput. Methods Appl. Mech. Eng.*, **284**, 807-834.
- Deng, J., Chen, F., Li, X., Hu, C., Tong, W., Yang, Z. and Feng, Y. (2008), "Polynomial splines over hierarchical T-meshes", *Graph. Models*, **70**, 76-86.
- Dokken, T., Lyche, T. and Pettersen, K.F. (2013), "Polynomial splines over locally refined box-partitions", *Comput. Aid. Geomet. Des.*, **30**(3), 331-356.
- Dörfler, M.R., Jüttler, B. and Simeon, B. (2010), "Adaptive isogeometric analysis by local h-refinement with T-splines", *Comput. Methods Appl. Mech. Eng.*, **199**(5), 264-275.
- Evans, E., Scott, M., Li, X. and Thomas, D. (2015), "Hierarchical T-splines: Analysis-suitability, Bézier extraction, and application as an adaptive basis for isogeometric analysis", *Comput. Methods Appl. Mech. Eng.*, **284**, 1-20.
- Flügge, S. and Truesdell, C. (1972), *Handbuch der Physik: Encyclopaedia of physics. vol. VIa/2, Mechanics of solids II. Festkörpermechanik II. Bd. VIa/2*: Springer-Verlag.
- Forsey, D.R. and Bartels, R.H. (1988), "Hierarchical B-spline refinement", *ACM Siggraph Computer Graphics*, **22**(4), 205-212.
- Giannelli, C., Jüttler, B. and Speleers, H. (2012), "THB-splines: The truncated basis for hierarchical splines", *Comput. Aid. Geomet. Des.*, **29**, 485-498.
- Giannelli, C., Jüttler, B., Kleiss, S.K., Mantzaflaris, A., Simeon, B. and Špeh, J. (2016), "THB-splines: An effective mathematical technology for adaptive refinement in geometric design and isogeometric analysis", *Comput. Methods Appl. Mech. Eng.*, **299**, 337-365.
- González, D., Cueto, E. and Doblaré, M. (2008), "Higher-order natural element methods: Towards an isogeometric meshless method", *Int. J. Numer. Method. Eng.*, **74**(13), 1928-1954.
- Hughes, T.J., Cottrell, J.A. and Bazilevs, Y. (2005), "Isogeometric analysis: CAD, finite elements, NURBS, exact geometry and mesh refinement", *Comput. Methods Appl. Mech. Eng.*, **194**(39), 4135-4195.
- Ivannikov, V., Tiago, C. and Pimenta, P. (2014), "On the boundary conditions of the geometrically nonlinear Kirchhoff-Love shell theory", *Int. J. Solids Struct.*, **51**(18), 3101-3112.
- Johannessen, K.A., Kvamsdal, T. and Dokken, T. (2014), "Isogeometric analysis using LR B-splines", *Comput. Methods Appl. Mech. Eng.*, **269**, 471-514.
- Johannessen, K.A., Remonato, F. and Kvamsdal, T. (2015), "On the similarities and differences between Classical Hierarchical, Truncated Hierarchical and LR B-splines", *Comput. Methods Appl. Mech. Eng.*, **291**, 64-101.
- Kang, P. and Youn, S.-K. (2016), "Isogeometric topology optimization of shell structures using trimmed NURBS surfaces", *Finite Elements in Analysis and Design*, **120**, 18-40.
- Khakalo, S. and Niiranen, J. (2017), "Isogeometric analysis of higher-order gradient elasticity by user elements of a commercial finite element software", *Comput.-Aid. Des.*, **82**, 154-169.
- Kiss, G., Giannelli, C., Zore, U., Jüttler, B., Großmann, D. and Barner, J. (2014), "Adaptive CAD model (re-) construction with THB-splines", *Graph. Models*, **76**, 273-288.
- Kraft, R. (1997), Adaptive and linearly independent multilevel B-splines: SFB 404, Geschäftsstelle.
- Lee, S.-W., Yoon, M. and Cho, S. (2017), "Isogeometric topological shape optimization using dual evolution with boundary integral equation and level sets", *Comput.-Aid. Des.*, **82**, 88-99.
- Li, X., Deng, J. and Chen, F. (2007), "Surface modeling with polynomial splines over hierarchical T-meshes", *The Visual Computer*, **23**(12), 1027-1033.
- Li, X., Zheng, J., Sederberg, T.W., Hughes, T.J. and Scott, M.A. (2012), "On linear independence of T-spline blending functions", *Comput. Aid. Geomet. Des.*, **29**(1), 63-76.
- Liu, G.-R. and Gu, Y. (2001), "A point interpolation method for two-dimensional solids", *Int. J. Numer. Methods Eng.*, **50**(4), 937-951.
- Liu, W.K., Jun, S. and Zhang, Y.F. (1995), "Reproducing kernel particle methods", *Int. J. Numer. Methods Fluids*, **20**(8-9), 1081-1106.
- Liu, H., Zhu, X. and Yang, D. (2016), "Isogeometric method based in-plane and out-of-plane free vibration analysis for Timoshenko curved beams", *Struct. Eng. Mech., Int. J.*, **59**(3), 503-526.
- Morgenstern, P. and Peterseim, D. (2015), "Analysis-suitable adaptive T-mesh refinement with linear complexity", *Comput. Aid. Geomet. Des.*, **34**, 50-66.
- Nguyen-Thanh, N., Kiendl, J., Nguyen-Xuan, H., Wüchner, R., Bletzinger, K., Bazilevs, Y. and Rabczuk, T. (2011a), "Rotation free isogeometric thin shell analysis using PHT-splines", *Comput. Methods Appl. Mech. Eng.*, **200**, 3410-3424.
- Nguyen-Thanh, N., Nguyen-Xuan, H., Bordas, S.P.A. and Rabczuk, T. (2011b), "Isogeometric analysis using polynomial splines over hierarchical T-meshes for two-dimensional elastic solids", *Comput. Methods Appl. Mech. Eng.*, **200**, 1892-1908.
- Riffnaller-Schiefer, A., Augsdörfer, U. and Fellner, D. (2016), "Isogeometric shell analysis with NURBS compatible subdivision surfaces", *Appl. Math. Computat.*, **272**, 139-147.
- Rosolen, A. and Arroyo, M. (2013), "Blending isogeometric analysis and local maximum entropy meshfree approximants", *Comput. Methods Appl. Mech. Eng.*, **264**, 95-107.
- Scott, M., Li, X., Sederberg, T. and Hughes, T. (2012), "Local refinement of analysis-suitable T-splines", *Comput. Methods Appl. Mech. Eng.*, **213**, 206-222.
- Sambridge, M., Braun, J. and McQueen, H. (1995), "Geophysical parametrization and interpolation of irregular data using natural neighbours", *Geophys. J. Int.*, **122**(3), 837-857.
- Schillinger, D., Dede, L., Scott, M.A., Evans, J.A., Borden, M.J., Rank, E. and Hughes, T.J. (2012), "An isogeometric design-through-analysis methodology based on adaptive hierarchical refinement of NURBS, immersed boundary methods, and T-spline CAD surfaces", *Comput. Methods Appl. Mech. Eng.*, **249**, 116-150.
- Sederberg, T.W., Zheng, J., Bakenov, A. and Nasri, A. (2003), "T-splines and T-NURCCs", In: *ACM Transactions on Graphics (TOG)*, ACM, pp. 477-484.
- Sederberg, T.W., Cardon, D.L., Finnigan, G.T., North, N.S., Zheng, J. and Lyche, T. (2004), "T-spline simplification and local refinement", In: *Acem Transactions on Graphics (tog)*, ACM, pp. 276-283.
- Seo, Y.-D., Kim, H.-J. and Youn, S.-K. (2010), "Shape optimization and its extension to topological design based on isogeometric analysis", *Int. J. Solids Struct.*, **47**(11), 1618-1640.
- Shojaee, S., Ghelichi, M. and Izadpanah, E. (2013), "Combination of isogeometric analysis and extended finite element in linear crack analysis", *Struct. Eng. Mech., Int. J.*, **48**(1), 125-150.
- Somireddy, M. and Rajagopal, A. (2014), "Meshless natural

- neighbor Galerkin method for the bending and vibration analysis of composite plates”, *Compos. Struct.*, **111**, 138-146.
- Tagliabue, A., Dedè, L. and Quarteroni, A. (2014), “Isogeometric analysis and error estimates for high order partial differential equations in fluid dynamics”, *Comput. Fluids*, **102**, 277-303.
- Taheri, A.H., Hassani, B. and Moghaddam, N. (2014), “Thermo-elastic optimization of material distribution of functionally graded structures by an isogeometrical approach”, *Int. J. Solids Struct.*, **51**(2), 416-429.
- Uhm, T.K. and Youn, S.K. (2009), “T-spline finite element method for the analysis of shell structures”, *Int. J. Numer. Method. Eng.*, **80**(4), 507-536.
- unther Greiner, G. and Hormann, K. (1996), “Interpolating and approximating scattered 3D-data with hierarchical tensor product B-splines”, In: *Proceedings of Chamonix*, pp. 1.
- Valizadeh, N., Bazilevs, Y., Chen, J. and Rabczuk, T. (2015), “A coupled IGA–Meshfree discretization of arbitrary order of accuracy and without global geometry parameterization”, *Comput. Methods Appl. Mech. Eng.*, **293**, 20-37.
- Vuong, A.-V., Giannelli, C., Jüttler, B. and Simeon, B. (2011), “A hierarchical approach to adaptive local refinement in isogeometric analysis”, *Comput. Methods Appl. Mech. Eng.*, **200**, 3554-3567.
- Wang, P., Xu, J., Deng, J. and Chen, F. (2011), “Adaptive isogeometric analysis using rational PHT-splines”, *Comput.-Aid. Des.*, **43**, 1438-1448.
- Wawrzinek, A., Hildebrandt, K. and Polthier, K. (2011), “Koiter’s Thin Shells on Catmull-Clark Limit Surfaces”, In: *VMV*, pp. 113-120.
- Wei, X., Zhang, Y., Hughes, T.J. and Scott, M.A. (2015), “Truncated hierarchical Catmull–Clark subdivision with local refinement”, *Comput. Methods Appl. Mech. Eng.*, **291**, 1-20.
- Willberg, C. (2016), “Analysis of the dynamical behavior of piezoceramic actuators using piezoelectric isogeometric finite elements”, *Adv. Computat. Des., Int. J.*, **1**(1), 37-60.
- Zore, U. and Jüttler, B. (2014), “Adaptively refined multilevel spline spaces from generating systems”, *Comput. Aid. Geomet. Des.*, **31**, 545-566.